Applied Numerical Mathematics 10 (1992) 335–355
North-Holland

APNUM350

Computations of blow-up and decay for periodic solutions of the generalized Korteweg–de Vries–Burgers equation *

Jerry L. Bona

Department of Mathematics and Applied Research Laboratory, The Pennsylvania State University, University Park, PA 16802, USA

Vassilios A. Dougalis

Department of Mathematics, National Technical University, Zographou, 15773 Athens, Greece

Ohannes A. Karakashian

Department of Mathematics, University of Tennessee, Knoxville, TN 37996, USA

William R. McKinney

Department of Mathematics, North Carolina State University, Raleigh, NC 27695, USA

Abstract

Bona, J.L., V.A. Dougalis, O.A. Karakashian and W.R. McKinney, Computations of blow-up and decay for periodic solutions of the generalized Korteweg–de Vries–Burgers equation, Applied Numerical Mathematics 10 (1992) 335–355.

A numerical scheme is suggested, discussed, and implemented for the approximation of solutions to the periodic initial-value problem for the generalized Korteweg–de Vries–Burgers equation. The resulting computer code is used to study singularity formation and other aspects of the interaction between nonlinearity, dispersion, and dissipation that is the hallmark of these evolutionary equations. It is found that unless the coefficient specifying the strength of the dissipation is large enough, initial data may lead to solutions that lose smoothness in finite time in exactly the same way as do solutions of the dissipationless equation.

Correspondence to: W.R. McKinney, Department of Mathematics, North Carolina State University, Raleigh, NC 27695-8205, USA. Telephone: (919) 515-3265. E-mail: mckinney@newton.math.ncsu.edu.

* Work supported in part by the Institute of Applied and Computational Mathematics of the Research Center of Crete, Iraklion, Crete, Greece, the National Science Foundation, USA, and the Science Alliance, University of Tennessee.

1. Introduction

This paper is a companion to another by the same authors [10], and aims to cast light on issues that arise naturally from this earlier study. In the previous effort, numerical methods were described, analyzed and implemented for the approximation of solutions to the periodic initial-value problem for the so-called generalized Korteweg–de Vries (GKdV) equation

$$u_t + u^p u_x + \varepsilon u_{xxx} = 0. \tag{1.1}$$

Here p is a positive integer and $u = u(x, t)$ is a real-valued function of the real variables x and t which is periodic in its first argument with period 1, say. In most applications u represents wave amplitude or some similar physical quantity, x represents distance in the principal direction of propagation of the waves, and t is proportional to elapsed time. In consequence, we will often refer to the independent variables x and t as the spatial and temporal variable, respectively. It is our purpose here to extend the numerical methods put forward in [10] to encompass approximations of solutions to the generalized Korteweg–de Vries–Burgers (GKdVB) equation

$$u_t + u^p u_x - \delta u_{xx} + \varepsilon u_{xxx} = 0, \tag{1.2}$$

augmented with the initial condition

$$u(x, 0) = u^0(x), \tag{1.3}$$

where u^0 is a given, periodic function with period 1, say.

Equation (1.2) is one of the simplest evolution equations that features nonlinearity, dissipation, and dispersion. The special case $p = 1$ and $\delta = 0$ is the classical Korteweg–de Vries (KdV) equation which arises in modeling many practical situations involving wave propagation in nonlinear dispersive media (cf. Benjamin [5], Jeffrey and Kakutani [17], or Scott, Chu and McLaughlin [24]). The Korteweg–de Vries–Burgers (KdVB) equation ((1.2) with $p = 1$ and $\delta, \varepsilon > 0$) is also frequently put forward when there is a need to take account of dissipative effects in addition to nonlinearity and dispersion (cf. Bona, Pritchard and Scott [12], Grad and Hu [16], and Johnson [18,19]. The value $p = 2$ also arises in modeling interesting physical phenomena. Larger values of p could arise in principle (see the discussion of Benjamin, Bona and Mahony [6, Section 2]). More common is a quadratic or cubic nonlinearity combined with a dispersive term that is weaker than the second derivative. One example is the well-known Benjamin–Ono equation

$$u_t + uu_x - \varepsilon Hu_x = 0$$

or the Benjamin–Ono–Burgers equation

$$u_t + uu_x - \varepsilon Hu_x - \delta u_{xx} = 0,$$

where H connotes the Hilbert transform. Indeed, all of the foregoing are special instances of a broad class of models having the form

$$u_t + f(u)_x - \varepsilon Lu_x + \delta Mu = 0, \tag{1.4}$$

where L and M are Fourier multiplier operators defined by

$$\widehat{Lv}(\xi) = \alpha(\xi)\hat{v}(\xi), \qquad \widehat{Mv}(\xi) = \beta(\xi)\hat{v}(\xi),$$

α and β are positive, even functions, and $f:\mathbb{R}\to\mathbb{R}$ is a smooth function. The general class of evolution equations (1.4) has attracted attention lately (cf. Abdelouhab, Bona, Felland and Saut [1], Biler [7], Bona, Souganidis and Strauss [13] and Dix [15] as a natural environment in which to study the interaction between nonlinear, dispersive, and dissipative effects. It is of interest to study (1.4) for a wide range of f, α, and β, and this is a project currently in view. However, if one restricts attention to local equations where α and β are polynomials, then (1.2) presents itself as an interesting sequence of model equations wherein the level of dispersion and dissipation is fixed and the strength of the nonlinearity is varied according to the choice of the integer p.

The initial-value problem for (1.1) with data as in (1.3) is known to be locally well-posed in reasonable function classes (cf. Kato [21,22] or Schechter [23]). For $p<4$, the problem is globally well-posed in that smooth solutions of (1.1) corresponding to specified initial data u^0 exist for all $(x, t)\in\mathbb{R}\times\mathbb{R}$, and, moreover, the mapping that associates u to u^0 is continuous in certain precise senses. For $p\geqslant 4$, the same result holds, but only if the initial data u^0 is not too large. (For $p>4$ and small data, we know in fact that the situation is purely dispersive in a precise sense first delineated by Strauss [25].) However, for $p\geqslant 4$ and arbitary smooth data, it is an open question whether or not the initial-value problem for (1.1) is globally well-posed. Indeed, one of the tentative conclusions of our previous work [10] is that solutions of (1.1) for $p\geqslant 4$ may form singularities in finite time, so that the initial-value problem appears not to be globally well-posed for this range of p. There is other evidence to be recounted below that gives credence to the same conclusion of lack of well-posedness.

Taking the evidence for lack of well-posedness at face value, one might subscribe to the view that while nonlinearity overwhelms the smoothing effects of dispersion in (1.1) for $p\geqslant 4$, any realistic modeling of physical phenomena will feature dissipation and this might effectively limit the singularity formation observed in our earlier study. A natural context in which to seek information concerning this latter prospect is the GKdVB equation (1.2) with both ε and δ positive. For the inital-value problem (1.2)–(1.3), local well-posedness is easily established in the same way as for (1.1).

The plan of the paper is as follows. In the next section, the numerical scheme is presented and theory relating to the convergence of its solutions to solutions of the underlying partial differential equations is outlined. A method for automatic spatial and temporal refinement is then introduced. Section 3 makes use of a computer code implementing the numerical scheme together with the automatic grid refinement to study the question raised in the last paragraph. It transpires that sufficiently large values of δ do indeed inhibit singularity formation. Surprisingly, singularities appear still to form if δ lies below a certain critical value. This aspect is studied in some detail in the last section, and related theory is mentioned that partially confirms the conclusions drawn from the numerical experiments. Other interesting aspects of the confluence of nonlinearity, dispersion, and dissipation in the equation (1.2) are also touched upon in Section 4.

2. Numerical approximations

After a word about notation, the numerical techniques used to generate fully-discrete approximations to solutions of (1.1) and (1.2) are briefly described. The numerical methods consist of a Galerkin finite-element method with smooth periodic splines for the spatial discretization and implicit Runge–Kutta methods of Gauss–Legendre type for the temporal discretization. These schemes are well-suited to approximate smooth solutions of nonlinear partial differential equations due to their excellent stability properties and high rates of convergence in both the spatial and temporal variable. An algorithm for adaptive grid refinement in both space and time is also presented which enables accurate numerical simulations of both (1.1) and (1.2) that indicate solutions form singularities in finite time. In the sequel, attention will be given mainly to numerical solutions of (1.2), making reference to (1.1) whenever it is appropriate.

The notation to be used is mostly standard. For positive real numbers $q \geqslant 1$, L_q will denote the collection of periodic functions of period 1 which are qth-power integrable on [0, 1] endowed with the norm

$$|f|_q = \left[\int_0^1 |f(x)|^q \, dx\right]^{1/q}.$$

The usual modification applies if $q = \infty$ and the norm on L_∞ is denoted by $|\cdot|_\infty$. For nonnegative integers s, H^s will denote the standard Hilbert space consisting of 1-periodic functions which, along with their first s derivatives are in L_2. The standard norm on H^s is denoted by $\|\cdot\|_s$. In addition, the norm and inner product of L_2 appear quite frequently and both will be written unadorned as $\|\cdot\|$ and $(\cdot, \cdot)$, respectively.

Let $r \geqslant 3$ be an integer and $S_h = S_h^r$ be the space of 1-periodic smooth splines of order r (polynomials of degree $r-1$) defined on a uniform partition of [0, 1] with mesh length $h = 1/N$ where N is a positive integer. It is well known that if v is a sufficiently smooth periodic function with period 1, then there exists a $\chi \in S_h$ such that for $1 \leqslant m \leqslant r$,

$$\sum_{j=0}^{m-1} h^j \| v - \chi \|_j \leqslant c h^m \| v \|_m, \tag{2.1}$$

where c is a constant independent of h, v, and χ. In addition to the above *approximation* properties, the finite-dimensional spaces S_h also possess the following *inverse* properties. There exists a constant c, independent of h, such that for all $\chi \in S_h$,

$$\| \chi \|_\beta \leqslant c h^{-(\beta-\alpha)} \| \chi \|_\alpha, \tag{2.2}$$

where $0 \leqslant \alpha \leqslant \beta \leqslant r-1$ and

$$|\chi|_\infty \leqslant c h^{-1/2} \| \chi \|. \tag{2.3}$$

The Galerkin semidiscrete approximation of the solution $u(x, t)$ of (1.2) is defined as a differentiable map $u_h : [0, T] \to S_h$ satisfying the relations

$$(u_{ht} + u_h^p u_{hx}, \chi) - (\varepsilon u_{hxx} - \delta u_{hx}, \chi_x) = 0, \quad \forall \chi \in S_h, \tag{2.4}$$

and

$$u_h(0) = \pi_h u^0, \tag{2.5}$$

where $\pi_h u^0$ denotes a conveniently chosen element of S_h (e.g. L_2-projection, interpolant, etc.) such that

$$\| \pi_h u^0 - u^0 \| \leqslant c h^r. \tag{2.6}$$

One may then prove, along the lines of the analogous proof for the KdV equation in [4], that if $u(x, t)$ is sufficiently smooth over a given time interval $[0, T]$, then u_h exists, is unique, and satisfies the error estimate

$$\max_{0 \leqslant t \leqslant T} \| u_h(t) - u(\cdot, t) \| \leqslant ch^r, \tag{2.7}$$

where c is a constant independent of h. Furthermore, letting $\chi = u_h$ in (2.4), integrating by parts and invoking periodicity to assure the boundary terms cancel, it is easy to see that

$$\| u_h(t) \| \leqslant \| u_h(0) \|, \quad t \geqslant 0. \tag{2.8}$$

Note that for equation (1.1), the inequality (2.8) is replaced by the strict equality

$$\| u_h(t) \| = \| u_h(0) \|, \quad t \geqslant 0. \tag{2.9}$$

Upon choosing a basis for S_h and representing u_h in terms of this basis, it is standard to view (2.4) as an initial-value problem for a system of N ordinary differential equations. Defining $F: S_h \to S_h$ by

$$(F(v), \chi) = -(v^p v_x, \chi) + (\varepsilon v_{xx} - \delta v_x, \chi_x), \tag{2.10}$$

allows this system of ordinary differential equations to be written in the compact form

$$\begin{cases} u_{ht} = F(u_h), & 0 \leqslant t \leqslant T, \\ u_h(0) = \pi_h u^0. \end{cases} \tag{2.11}$$

To obtain the fully-discrete approximations, one may now choose from a variety of numerical methods for solving initial-value problems for systems of ordinary differential equations. In the nondissipative case ($\delta = 0$) corresponding to (1.1), our previous work [10] focused on discretizing the system (2.11) in time via a class of implicit Runge–Kutta methods of Gauss–Legendre type. These methods were selected because of their excellent stability properties and high rate of convergence. In addition, they are conservative, a property that is necessary for the existence of a discrete conservation law similar to (2.9). Although the evolution equation (1.2) is not conservative, the dissipative aspect presents no obvious difficulties for the suggested, high-order accurate numerical methods.

In the light of the remarks in the last paragraph, a q-stage Gauss–Legendre method was applied to the system (2.11). For integer $J > 0$, let $t^n = nk$, $n = 0, 1, \ldots, J$, where the step size is given by $k = T/J$. Approximations $u_h^n \in S_h$ to the true solution $u(\cdot, t^n)$ of (1.2) are defined by letting $u_h^0 = \pi_h u^0$, and for $n = 0, 1, \ldots, J-1$,

$$u_h^{n+1} = u_h^n + k \sum_{i=1}^{q} b_i F(u_h^{n,i}), \tag{2.12}$$

where the intermediate values $u_h^{n,i}$, $i = 1, \ldots, q$, are the solutions of the system of qN nonlinear equations

$$u_h^{n,i} = u_h^n + k \sum_{j=1}^{q} a_{ij} F(u_h^{n,j}). \tag{2.13}$$

In the numerical experiments presented herein, we restricted ourselves to the two-stage Gauss–Legendre method for which the constants a_{ij} and b_i for $1 \leqslant i, j \leqslant 2$ are given by the tableau

$$\frac{\begin{matrix} a_{11} & a_{12} \\ a_{21} & a_{22} \end{matrix}}{\begin{matrix} b_1 & b_2 \end{matrix}} = \frac{\begin{matrix} 1/4 & 1/4-\beta \\ 1/4+\beta & 1/4 \end{matrix}}{\begin{matrix} 1/2 & 1/2 \end{matrix}},$$

where $\beta = 1/\sqrt{12}$. In this case, (2.13) is a nonlinear system of $2N$ equations that may be decoupled and solved using a Newton-type iteration as described in [9,10]. The following result is straightforward to demonstrate for any of the time-stepping schemes mentioned above.

Proposition 2.1. *For $n = 0, 1, \ldots, J-1$, the equations (2.12) and (2.13) have solutions $u_h^{n+1} \in S_h$ and $u_h^{n,i} \in S_h$, $i = 1, \ldots, q$. Furthermore,*

$$\| u_h^n \| \leqslant \| \pi_h u^0 \| \quad \text{for } n = 0, 1, \ldots, J. \tag{2.14}$$

The above proposition demonstrates that the fully-discrete approximations are stable in L_2. It may be proved using the same techniques as in [10, Propositions 3.1 and 3.2]. For equation (1.1), (2.14) holds with equality, and this provides a fully-discrete analog of the second invariant of the GKdV equation and of the semidiscrete result (2.9). The following theorem shows that the optimal temporal rate of convergence $2q$ is achieved for a q-stage Gauss–Legendre method. It may be demonstrated by generalizing the proof contained in [20] for the KdV equation itself ($p = 1$, $\delta = 0$).

Theorem 2.2. *Assume that $u^0(x)$ is smooth enough to guarantee the existence and necessary smoothness of the solution $u(x, t)$ for $0 \leqslant t \leqslant T$. If k and h are sufficiently small, and if $u_h^0 = \pi_h u^0$ satisfies (2.6), then for $n = 0, 1, \ldots, J$, there exists a unique solution u_h^n of (2.12) and (2.13) such that*

$$\max_{0 \leqslant n \leqslant J} \| u_h^n - u(\cdot, t^n) \| \leqslant c(k^{2q} + h^r) \tag{2.15}$$

for some constant c independent of h and k.

Previous computational experiments with fixed h and k and $p \geqslant 4$ in (1.1), produced numerical approximations which were seen to grow until the L_∞-norm of the approximations was large enough to cause substantial numerical difficulties. Indeed, combining the $L_\infty - L_2$ inverse inequality in (2.3) and the stability result (2.14), it follows that for a uniform mesh

$$| u_h^n |_\infty \leqslant ch^{-1/2} \| u_h^n \| \leqslant ch^{-1/2} \| \pi_h u^0 \| \quad \text{for } n = 0, 1, \ldots, J. \tag{2.16}$$

In consequence, if one expects large values of a solution relative to its L_2-norm, one will need appropriately small values of h. In our preceding studies, solutions appeared to become unboundedly large and the possibility of making approximations with small enough values of h on a uniform grid became computationally intractable. Since a uniform grid is impractical if one is to simulate solutions of (1.1) or (1.2) that grow substantially in L_∞, an algorithm with automatic grid refinement was implemented so that one may approximate solutions that develop an arbitrarily large peak, and in fact form a singularity in L_∞ at some point (x^*, t^*). The adaptive mechanism in our code consists of three main parts:

(i) local refinement of the spatial grid,
(ii) local selection of a temporal step size k, and
(iii) spatial translations of the solution.

The spatial refinements consisted of adding new nodes, distributed evenly about the midpoint $x = 0.5$, but in successively smaller, nested neighborhoods of the midpoint. This local refinement is combined with (iii), which attempts to keep the peak of the numerical approximation near the midpoint in the region of highest density of nodes, and away from a region of coarse mesh. Part (iii) is accomplished by occasionally translating the solution and centering the peak at $x = 0.5$.

The particular choice of spatial refinement (i) is based on a local $L_\infty - L_2$ inverse property on the region of smallest mesh. Let Ω^* represent the neighborhood of the midpoint $x = 0.5$ which is the region with the finest grid, with grid size h^*. At each time step, compute

$$Z_\infty = |u_h^n|_\infty \quad \text{and} \quad Z_2 = \left[\int_{\Omega^*} (u_h^n)^2 \, dx\right]^{1/2}.$$

The grid is then refined, new nodes are added, and both Ω^* and h^* are cut in half if

$$\frac{Z_\infty \sqrt{h^*}}{Z_2} > \text{TOL}_1.$$

Values of TOL_1 in the range [0.15, 0.20] were found to be very effective.

For (ii), the temporal step size is adjusted in an attempt to preserve the third invariant of the GKdV equation. This invariant is the functional

$$I_3(v) = \int_0^1 \left[v^{p+2} - \tfrac{1}{2}(p+1)(p+2)\varepsilon(v_x)^2\right] dx.$$

For exact solutions $u(x, t)$ of (1.1), $I_3(u(\cdot, t)) = I_3(u^0)$ is independent of the value of t. Given u_h^n, a possible u_h^{n+1} is computed using the current step size k. It is accepted if

$$\frac{|I_3(u_h^{n+1}) - I_3(u_h^n)|}{\int_0^1 [(u_h^{n+1})_x]^2 \, dx} < \text{TOL}_2, \tag{2.17}$$

where TOL_2 is a small parameter. If (2.17) is not satisfied, then k is cut in half and the process is repeated until (2.17) is satisfied. Although I_3 is not an invariant of (1.2), it nevertheless proved effective to use (2.17) as a criterion to control the step size for the dissipative equation. In the results to be presented, we used $10^{-6} \leqslant \text{TOL}_2 \leqslant 10^{-5}$.

3. Numerical simulations of blow-up

In this section, use is made of an implementation of the numerical scheme described in Section 2 to study the issue raised in the Introduction of whether or not solutions of the initial-value problem (1.2)–(1.3) generally exist for all time.

It is known (see [2,22]) that solutions are global in time unless they blow up in the L_∞-norm in finite time; that is, global existence is contradicted if and only if there is a t^* such that

$$|u(\cdot, t)|_\infty \to \infty \quad \text{as } t \to t^*. \tag{3.1}$$

In our previous studies, [9,10], it was found that (3.1) apparently obtains for some solutions of (1.1) when $p \geqslant 4$. Indeed, not only was singularity formation observed, but it appeared from the numerical simulations that the blow-up took place via a similarity structure. This led us in our previous work to compute the rates of blow-up for various norms in an effort to assess how closely the singularity seemed to fit the conjectured similarity structure. The evidence in favor of this hypothesis was substantial.

We now seek to determine whether or not the dissipative effects rendered by having $\delta > 0$ effectively staunch the formation of singularities. It appears from our results that singularity formation may still occur even in the presence of damping. Examples of finite-time blow-up are given for both the dispersive equation (1.1) and the dispersive–dissipative equation (1.2). Also, for several different norms, rates at which the numerical solutions blow up are determined. These rates are computed for two different types of initial profiles and agree quite well with those that obtain for a possible similarity solution mentioned above that was inferred to be present in the nondissipative case. Here, we shall only consider the case $p = 5$; similar numerical results hold as well for other values of $p \geqslant 5$ (see [9,10]; the borderline case $p = 4$ proved to be somewhat more challenging to understand in the aspect under discussion).

We begin by considering the numerical approximation of the exact, solitary-wave solutions

$$u(x, t) = A \operatorname{sech}^{2/p}\left[K\left(x - \tfrac{1}{2}\right) - \omega t\right], \tag{3.2}$$

where

$$K = \sqrt{\frac{p^2 A^p}{2\varepsilon(p+1)(p+2)}}, \qquad \omega = \frac{2KA^p}{(p+1)(p+2)},$$

and A is the amplitude of the wave. Although (3.2) is an exact solution of the pure initial-value problem for (1.1) posed on the whole real line, if A/ε is sufficiently large, then it is also an approximate solution of the initial-boundary-value problem with periodic boundary conditions on [0, 1] since the tails of the solitary wave decay exponentially (see [8] for a discussion of the relation between the pure initial-value problem and the periodic initial-value problem).

It was proved in [13] that the solitary-wave solutions (3.1) of the pure initial-value problem for (1.1) are stable to perturbations of the initial data if and only if $p < 4$. Stability here is understood as orbital stability. As mentioned before, it is also known that the initial-value problem for (1.1) is globally well-posed if $p < 4$, but for $p \geqslant 4$ the available theory only shows well-posedness locally in time. These facts lead one to ask what happens to perturbations of an unstable solitary wave as time increases? This turns out to be related to the question posed earlier of whether or not (1.1) is globally well-posed if $p \geqslant 4$.

Our previous studies addressed the just-mentioned issues. The numerical experiments of Bona et al. [10] using cubic splines for the spatial discretization and the two-stage Gauss–Legendre method for the time-stepping in conjunction with the aforementioned adaptive procedure for refining the discretization parameters, indicated that the instability of the solitary wave manifests itself by transforming the solitary wave into a similarity solution that proceeds

Table 1
Blow-up rates, perturbed solitary wave, $p = 5$, $A = 2$, $\varepsilon = 5\times10^{-4}$, $\delta = 0$, $\lambda = 1.01$

i	L_4	L_5	L_6	L_7	L_∞	$L_{2,\mathrm{D}}$	$L_{\infty,\mathrm{D}}$
5	0.5029(−1)	0.6683(−1)	0.7795(−1)	0.8590(−1)	0.1336	0.3008	0.4657
10	0.5047(−1)	0.6729(−1)	0.7853(−1)	0.8657(−1)	0.1348	0.3028	0.4731
15	0.4983(−1)	0.6647(−1)	0.7759(−1)	0.8554(−1)	0.1334	0.2992	0.4618
20	0.4989(−1)	0.6658(−1)	0.7773(−1)	0.8572(−1)	0.1338	0.2999	0.4690
25	0.5044(−1)	0.6728(−1)	0.7851(−1)	0.8654(−1)	0.1347	0.3029	0.4747
30	0.4974(−1)	0.6633(−1)	0.7741(−1)	0.8534(−1)	0.1329	0.2985	0.4685
35	0.5001(−1)	0.6672(−1)	0.7786(−1)	0.8583(−1)	0.1336	0.3004	0.4654

to blow-up in L_∞ at some point (x^*, t^*) with $t^* < \infty$. For example, using as initial data the slightly perturbed solitary wave

$$u^0(x) = \lambda A\ \mathrm{sech}^{2/p}\left[K\left(x - \tfrac{1}{2}\right)\right] \tag{3.3}$$

in place of (3.1), with $p = 5$, $A = 2$, $\varepsilon = 5 \times 10^{-4}$, $\delta = 0$, and $\lambda = 1.01$, the adaptive strategy was able to refine the grid 42 times and allowed the numerical solution to reach a peak of over 200,000 with the point of blow-up being given by $x^* \approx 0.61333$ and $t^* \approx 0.022549$ (see [10]). Rates of blow-up of various L_q-norms of the solution and of the L_2- and L_∞-norm of its derivative (denoted by $L_{2,\mathrm{D}}$ and $L_{\infty,\mathrm{D}}$, respectively) were also computed for this particular solution. By a blow-up rate, we mean the positive numbers ρ such that

$$M(t) \sim (t^* - t)^{-\rho} \quad \text{as } t \to t^*,$$

where $M(t)$ is one of the just-mentioned norms. These rates were given in [10, Table 22] and are reproduced here in Table 1. For each row of Table 1, the value of i indicates the point in time at which the ith spatial refinement occurs; for details see [10]. These rates, along with similar rates from many other numerical experiments using different values of p support the conjecture that the solution blows up in the form

$$u(x, t) = \frac{1}{(t^* - t)^{2/3p}}\phi\left(\frac{x^* - x}{(t^* - t)^{1/3}}\right) + \text{bounded term}, \tag{3.4}$$

where $\phi(\xi)$ is a bounded function. For example, in Table 2 the rates at which the norms appearing in Table 1 blow up are given. The computed blow-up rates of the numerical solution in Table 1 agree quite well with the rates in Table 2 suggested by the conjectured solution-form (3.3). Since the conjectured solution evinces a strong singularity in finite time, it is natural to surmise that solutions of (1.1) will not exist for all $t > 0$.

In light of the above, it seemed interesting to carry out the same numerical experiments that had been effected previously for (1.1) on the initial-value problem for (1.2) with $\delta > 0$.

Table 2
Blow-up rates of conjectured similarity solution (3.3), $p = 5$

Norm	L_4	L_5	L_6	L_7	L_∞	$L_{2,\mathrm{D}}$	$L_{\infty,\mathrm{D}}$
Rate	0.500(−1)	0.667(−1)	0.778(−1)	0.857(−1)	0.133	0.300	0.467

Table 3
Blow-up rates, perturbed solitary wave, $p = 5$, $A = 2$, $\varepsilon = 5\times10^{-4}$, $\delta = 2\times10^{-4}$, $\lambda = 1.01$

i	L_4	L_5	L_6	L_7	L_∞	$L_{2,\mathrm{D}}$	$L_{\infty,\mathrm{D}}$
5	0.5049(−1)	0.6700(−1)	0.7814(−1)	0.8612(−1)	0.1341	0.3009	0.4639
10	0.4995(−1)	0.6655(−1)	0.7763(−1)	0.8555(−1)	0.1331	0.2994	0.4594
15	0.5000(−1)	0.6670(−1)	0.7787(−1)	0.8586(−1)	0.1339	0.3004	0.4660
20	0.4987(−1)	0.6645(−1)	0.7747(−1)	0.8533(−1)	0.1325	0.2988	0.4598
25	0.5012(−1)	0.6688(−1)	0.7808(−1)	0.8609(−1)	0.1343	0.3012	0.4683
30	0.5012(−1)	0.6681(−1)	0.7793(−1)	0.8587(−1)	0.1334	0.3006	0.4720
35	0.5007(−1)	0.6675(−1)	0.7786(−1)	0.8579(−1)	0.1333	0.3003	0.4665

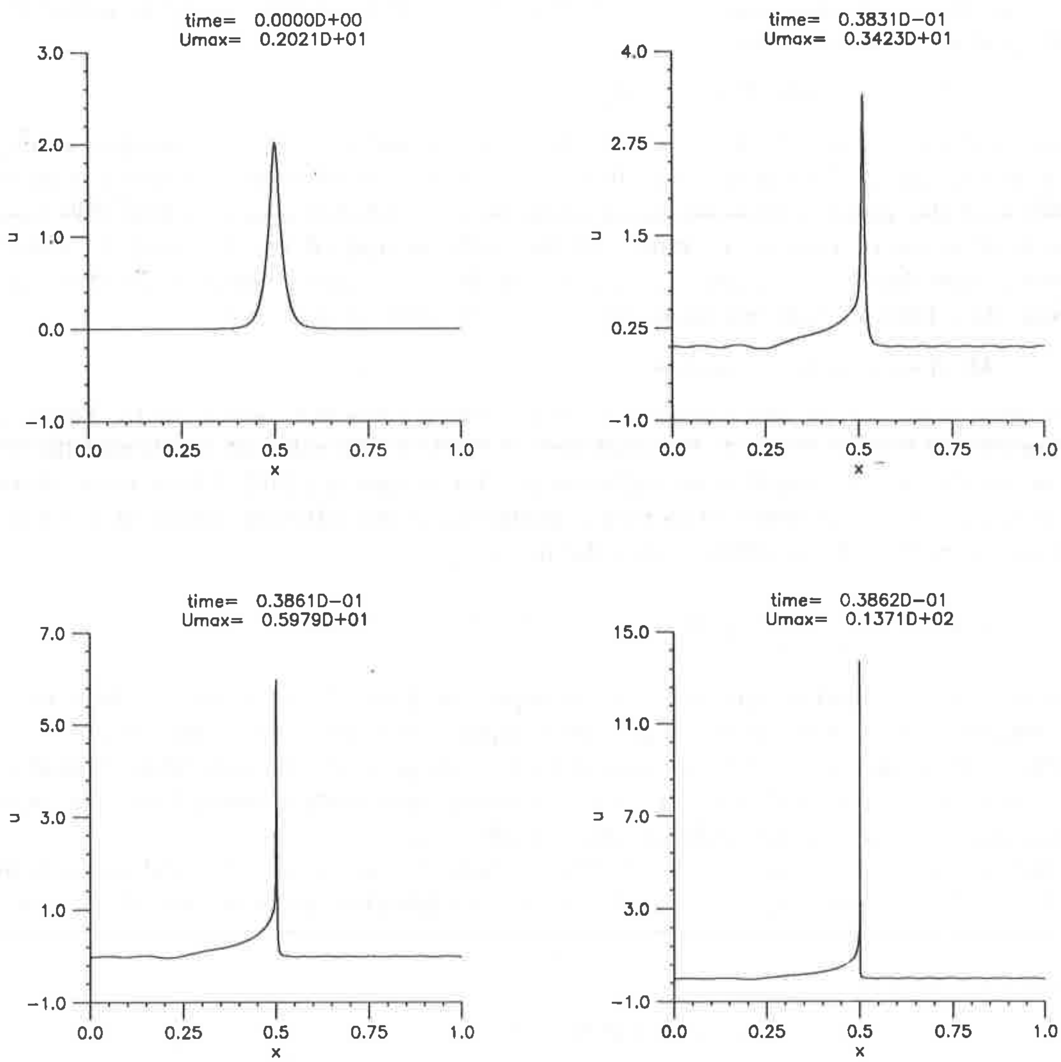

Fig. 1(a). Numerical blow-up of a perturbed solitary-wave solution with $p = 5$, $A = 2$, $\varepsilon = 5\times10^{-4}$, $\delta = 2\times10^{-4}$, $\lambda = 1.01$.

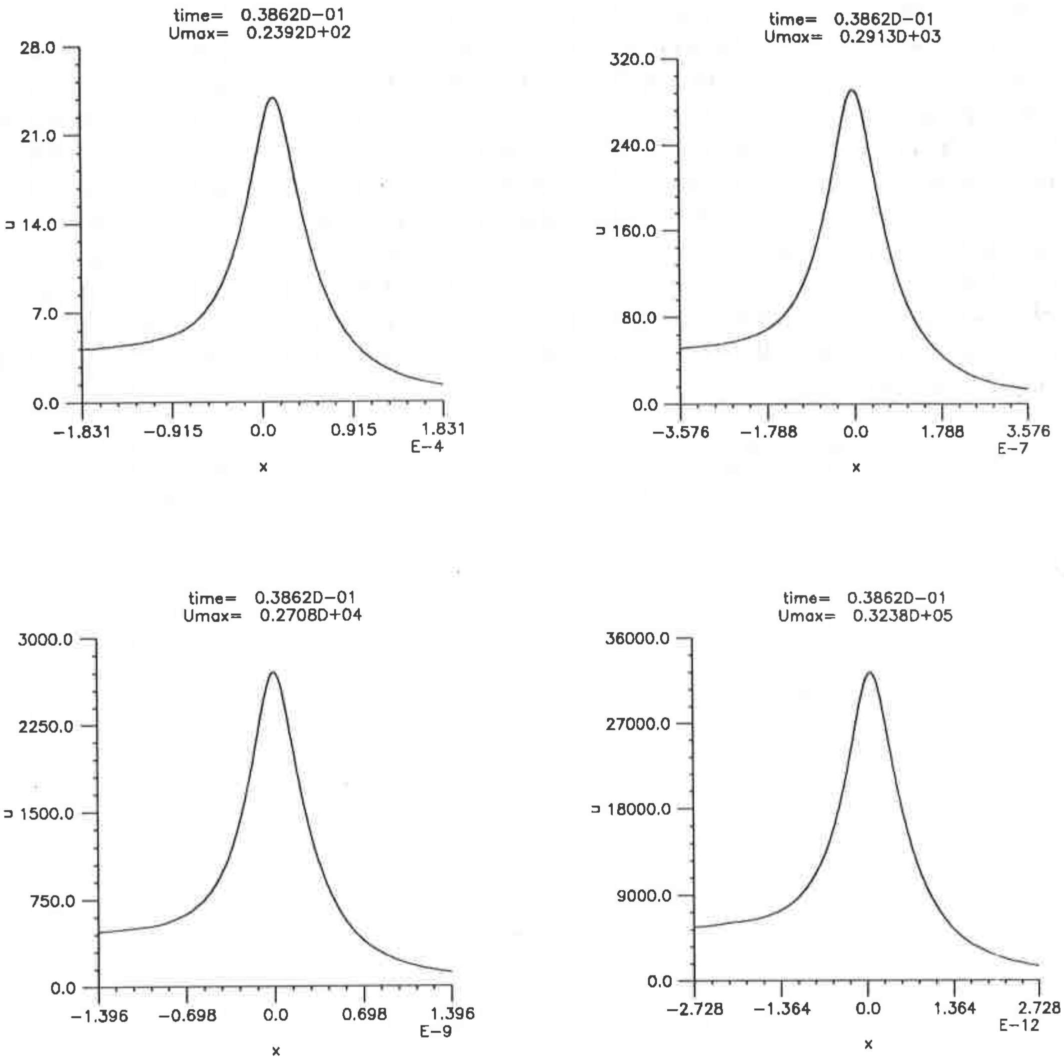

Fig. 1(b). Profile of the peak for the continuation of the integration of the perturbed solitary-wave solution with $p=5$, $A=2$, $\varepsilon=5\times10^{-4}$, $\delta=2\times10^{-4}$, $\lambda=1.01$.

Repeating the run of Table 1 but with a small amount of dissipation added ($p=5$, $A=2$, $\varepsilon=5\times10^{-4}$, $\delta=2\times10^{-4}$, $\lambda=1.01$), the peak of the numerical solution again increased several orders of magnitude. The blow-up rates for this approximation are provided in Table 3 and are very similar to those in Table 1. Thus it seems solutions of (1.2) can blow up, provided the dissipation is small enough. Although the dissipation did not appear to have any effect on the blow-up rates, it is worth to remark that it did delay the blow-up, as the singular point was, in this instance, $x^* \approx 0.65812$ and $t^* \approx 0.038624$. In the next section, it will be seen that with a sufficiently large amount of dissipation there is no longer blow-up, and in fact the solution will be seen to decay in this case.

To give a better idea of the structure and behaviour of the solution as it forms a singularity, the graph of the numerical solution for the dissipative problem is depicted at several different times in Fig. 1. In Fig. 1(a), as the peak U_{max} increases, the vertical axis is scaled in order that the entire profile may be shown. This causes the solution to appear to be very small except at the peak, which is always near $x = 0.5$ due to the translations that are part (iii) of our adaptive numerical scheme. A more detailed look at the structure of the solution near the peak is provided in Fig. 1(b), where both the horizontal and vertical axes are scaled. These plots are of the solution on the region of finest mesh Ω^*, with both the solution and region Ω^* being translated by $-\frac{1}{2}$ so that the peak is located near zero. The plots in Fig. 1(b) strongly indicate that the blow-up is of a self-similar type. We remark that our code was able to continue until the grid had been refined 40 times so that the smallest mesh size was $h^* \approx 10^{-14}$ and the step size had decreased to $k \approx 10^{-38}$.

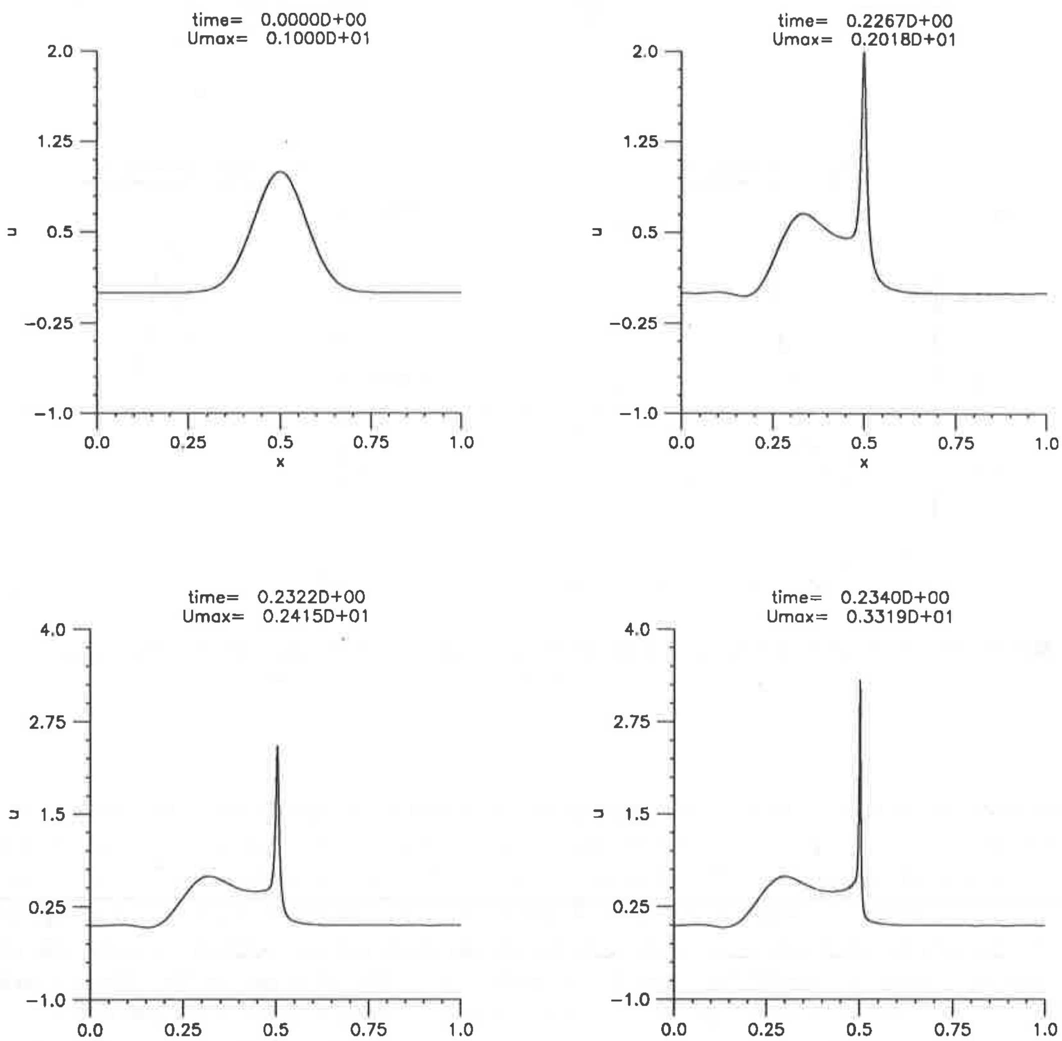

Fig. 2(a). Numerical simulation of blow-up from a Gaussian profile with $p = 5$, $\varepsilon = 1.21 \times 10^{-4}$, $\delta = 0$.

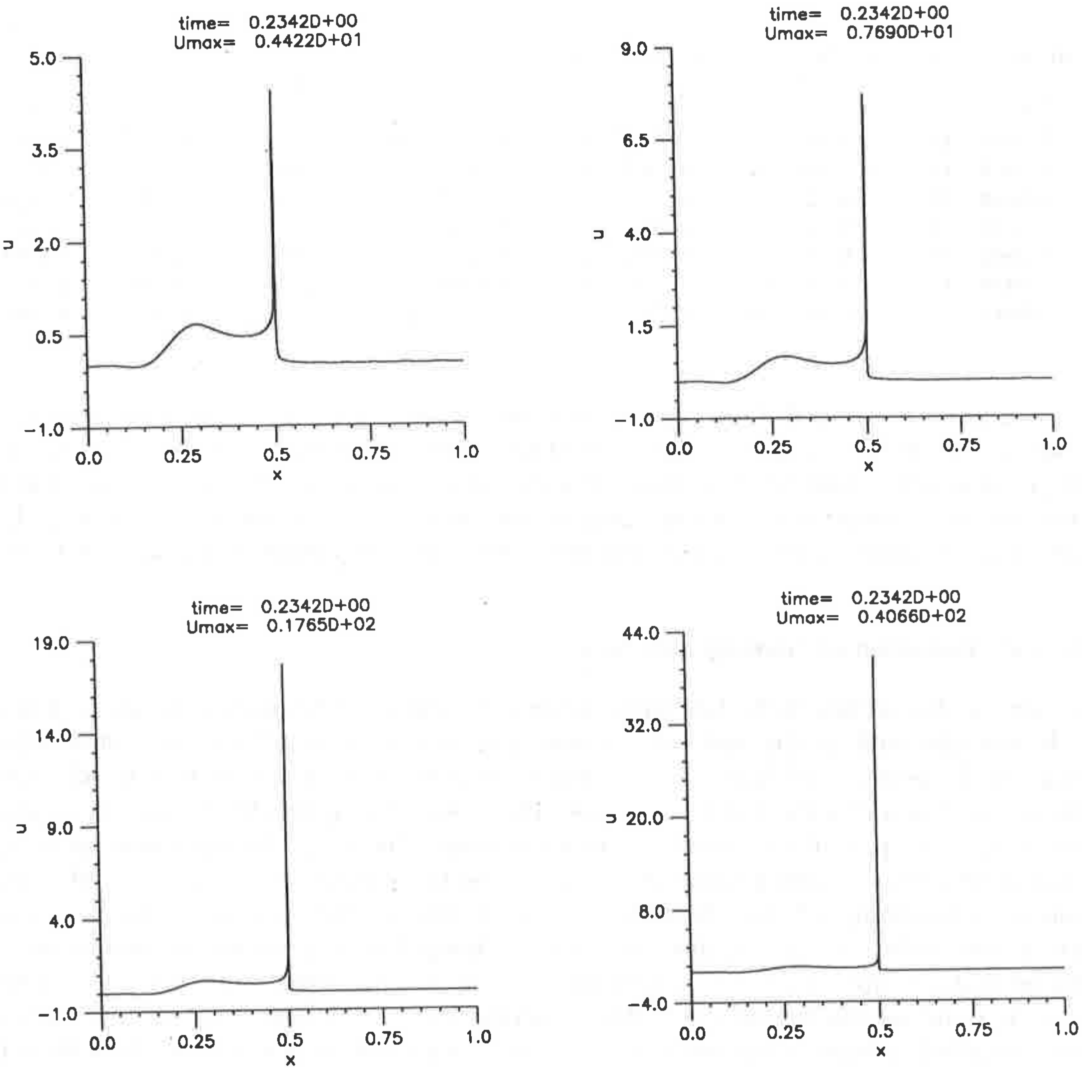

Fig. 2(b). Continued numerical simulation of blow-up from a Gaussian profile with $p = 5$, $\varepsilon = 1.21 \times 10^{-4}$, $\delta = 0$.

In another set of experiments, we used Gaussian profiles

$$u^0(x) = \mathrm{e}^{-100(x-1/2)^2} \tag{3.5}$$

as our initial conditions. The outcome of a run with $p = 5$, $\varepsilon = 1.21 \times 10^{-4}$, $\delta = 0$ is pictured in Fig. 2. As is apparent upon inspection of the graphs of the numerical approximations of the solution, a solitary wave separated rapidly from the bulk of the initial data. After emerging, the solitary wave evinced the instability predicted by the aforementioned theory, and rapidly formed a singularity. Adding dissipation to the problem with a Gaussian initial profile (the parameters for the equation were $p = 5$, $\varepsilon = 2 \times 10^{-4}$, $\delta = 10^{-4}$) led to very similar behaviour of the numerical solution. The rates of blow-up for the case where $\delta = 10^{-4}$ with initial data as

Table 4
Blow-up rates, Gaussian profile, $p=5$, $\varepsilon=2\times10^{-4}$, $\delta=10^{-4}$

i	L_4	L_5	L_6	L_7	L_∞	$L_{2,\mathrm{D}}$	$L_{\infty,\mathrm{D}}$
5	0.4986(−1)	0.6653(−1)	0.7761(−1)	0.8551(−1)	0.1329	0.2990	0.4655
10	0.5013(−1)	0.6687(−1)	0.7803(−1)	0.8600(−1)	0.1340	0.3010	0.4722
15	0.5000(−1)	0.6667(−1)	0.7778(−1)	0.8572(−1)	0.1333	0.3000	0.4676
20	0.5007(−1)	0.6678(−1)	0.7792(−1)	0.8588(−1)	0.1337	0.3005	0.4697
25	0.4986(−1)	0.6647(−1)	0.7755(−1)	0.8547(−1)	0.1330	0.2992	0.4653
30	0.5008(−1)	0.6677(−1)	0.7788(−1)	0.8582(−1)	0.1335	0.3004	0.4702
35	0.5009(−1)	0.6678(−1)	0.7791(−1)	0.8587(−1)	0.1337	0.3005	0.4684

in (3.5) are given in Table 4. Once again, the rates for this particular experiment appear to be very close to the blow-up rates for the conjectured similarity solution. This leads us to surmise that if $p \geqslant 4$ and the initial data is large enough, then even in the presence of dissipation the solution will be dominated by an emerging solitary wave which, upon establishing itself as a spatially separate entity, becomes unstable and blows up in the manner indicated in (3.4).

4. Effect of dissipation on blow-up and decay

The aim of this section is to determine further the effect of dissipation on the solutions of (1.2). It was observed in the last section that with relatively small amounts of dissipation, solutions of the generalized Korteweg–de Vries–Burgers equation could blow up in a fashion similar to that found for the GKdV equation. Here, we investigate the amount of dissipation necessary so that (perturbed) solitary waves no longer blow up. In particular, it is shown numerically that there exists a threshold value C_* of the parameter $C=\delta^2/\varepsilon A^p$ that plays a key role in determining whether there is blow-up or decay. (The ratio δ^2/ε has been studied previously and in the case $p=1$, this ratio may be thought of as a scaling parameter for (1.2).) It is found that for values of $C<C_*$, solutions blow up in finite time, while if $C>C_*$ solutions are bounded and persist for all $t>0$. The experiments on which we base this last assertion, namely perturbed solitary waves with $\lambda=1.01$, are somewhat narrow, but we feel them to be representative. The context of perturbed solitary waves was indicated in the last section to have broader applicability than one might expect because of the distinguished role played by these waveforms in the evolution of arbitrary initial data. It transpires that if a solution does not form singularities, then it decays in a manner similar to that of 1-periodic solutions of the linear equation $u_t-\delta u_{xx}+\varepsilon u_{xxx}=0$.

Table 5
Determination of δ_* for $A=2$, $p=5$

ε	δ_*^-	δ_*^+	δ_*
0.10(−3)	0.10(−3)	0.11(−3)	0.105(−3)
0.25(−3)	0.16(−3)	0.17(−3)	0.165(−3)
0.50(−3)	0.230(−3)	0.235(−3)	0.2325(−3)
0.80(−3)	0.28(−3)	0.30(−3)	0.290(−3)

Table 6
Critical values of δ_* and δ_*^2/ε, for $A=2$, $p=5, 6$

ε	$p=5$		$p=6$	
	δ_*	δ_*^2/ε	δ_*	δ_*^2/ε
0.10(−3)	0.105(−3)	0.110(−3)	0.275(−3)	0.756(−3)
0.25(−3)	0.165(−3)	0.109(−3)	0.435(−3)	0.757(−3)
0.50(−3)	0.233(−3)	0.108(−3)	0.625(−3)	0.781(−3)
0.80(−3)	0.290(−3)	0.106(−3)	0.785(−3)	0.770(−3)

This set of experiments begins by specifying p and initial (perturbed) solitary-wave profiles (3.2) with $A=2$ and $\lambda=1.01$. For each ε, the dissipative parameter δ is varied until two values δ_*^- and δ_*^+ are selected by experimentation for which one has (i) if $\delta \leqslant \delta_*^-$, then there is "definite" blow-up and (ii) if $\delta \geqslant \delta_*^+$, then there is "definite" decay. The quantity δ_* is then defined to be the average of δ_*^- and δ_*^+. The results of one set of experiments are presented in Table 5.

The critical values of δ_* are contained in Table 6 wherein the values of the ratios δ_*^2/ε are also shown. It is clear from this table that for fixed A and p, the critical value of δ_*^2/ε (that determines if there is blow-up or global existence and decay) is independent of ε.

To get an idea of the dependence of δ_* on A and p, the quantity ε was fixed at the value $\varepsilon = 0.5\times 10^{-3}$ and the amplitude A was varied. This was done for $p=5$ and $p=6$. For each new value of A, the critical value of δ_*^2/ε must be computed for $p=5,6$. The results of these computations are shown along with the associated parameter $C_* = \delta_*^2/\varepsilon A^p$ in Table 7.

The numerical evidence in these tables leads to the following conjecture.

Conjecture. *There is a critical value C_* of the parameter $C=\delta^2/\varepsilon A^p$ such that if C is greater than C_*, then the corresponding solution of* (1.2) *with the perturbed solitary wave* ($\lambda = 1.01$) *as initial value will exist for all t. On the other hand, if C is less than C_*, the solution will blow up in finite time.*

Of course the value of C_* will depend on the initial profile. As one sees from Table 7, for the initial condition (3.2) we have $C_* \approx 0.34\times 10^{-5}$ if $p=5$ and $C_* \approx 1.22\times 10^{-5}$ if $p=6$. While not reported in the tables, the value of C_* corresponding to $p=7$ has been determined to be $C_* \approx 2.42\times 10^{-5}$, thus showing a not unexpected nonlinear dependence of C_* on p.

Table 7
Critical values of δ_*^2/ε and $C_* = \delta_*^2/\varepsilon A^p$, for $\varepsilon = 5\times 10^{-4}$, $p=5, 6$

A	$p=5$		$p=6$	
	δ_*^2/ε	C_*	δ_*^2/ε	C_*
1.5	0.026(−3)	0.348(−5)	0.140(−3)	1.233(−5)
2.0	0.108(−3)	0.338(−5)	0.781(−3)	1.221(−5)
2.5	0.328(−3)	0.336(−5)	2.952(−3)	1.209(−5)
3.0	0.832(−3)	0.342(−5)	8.862(−3)	1.216(−5)

One can go further in interpreting the foregoing results. As discussed already, certain general classes of initial conditions evolve into solitary waves and a dispersive tail, albeit slowly modified by the damping term. One would expect that if the largest solitary wave that emerges from the given initial data has an amplitude A, then for δ large enough to guarantee that this size solitary wave is damped sufficiently to produce global existence, there should be a global solution corresponding to this data. Conversely, if δ is such that the corresponding value of C is below the critical value, then it is expected that such initial data will lead to blow up in finite time. The last statement is probably not valid in such a simple form because other numerical experiments show that the value of C_* for a perturbed solitary wave depends on the direction in function space of the perturbation as well as on the other parameters A, ε, and δ.

A more detailed study of the boundary between blow-up and decay will be presented in a forthcoming work by the present authors [11]. In this work, we prove a theorem stating that if the dissipation is sufficiently large compared to the initial condition u^0, then the solution of (1.2) will exist globally. Moreover, our theorem yields an estimate on the size of δ that has exactly the parameter dependence manifested in our definition of C_*. An immediate consequence of the dissipation being large enough to guarantee global existence is the following decay result which is valid for any value of p.

Proposition 4.1. *Assume the data of the problem* (1.2) *to be such that the solution is smooth and exists for all* t. *Then*

$$\| u(t) - u^* \| \leqslant e^{-4\pi^2 t} \| u^0 - u^* \| \tag{4.1}$$

where $u^* = \int_0^1 u^0(x)\,dx$.

Remark 4.2.

(1) Biler [7] has obtained detailed decay estimates for periodic solutions in the case $p < 2$.

(2) This proposition shows that as $t \to +\infty$ global periodic solutions of (1.2) approach a constant function which is determined by their initial value, at an exponential rate in the L_2-norm.

(3) This result is in marked contrast to the situation that obtains for global solutions of the pure initial-value problem for (1.2). Solutions corresponding to Sobolev-class H^s-initial data are expected to decay to zero as $t \to +\infty$. However, the rate of decay is only algebraic in t as witnessed by the results of Amick, Bona and Schonbek [3] where for $p = 1$ it was shown that

$$\int_{-\infty}^{\infty} u^2(x, t)\,dx = O(t^{-1/2}),$$

and that this rate is sharp in general.

Proof of Proposition 4.1. Let $v = u - u^*$. Then for all $t \geqslant 0$, $v(\cdot, t)$ has mean-value zero, is 1-periodic, and satisfies the equation

$$v_t + (v + u^*)^p v_x - \delta v_{xx} + \varepsilon v_{xxx} = 0. \tag{4.2}$$

Since u^* is constant, taking the inner product of (4.2) with v, integrating by parts and using periodicity yields

$$\frac{\mathrm{d}}{\mathrm{d}t}\| v \|^2 + 2\delta \| v_x \|^2 = 0. \tag{4.3}$$

Because v is a 1-periodic function with mean value zero, it follows that $\| v \| \leqslant (2\pi)^{-1} \| v_x \|$. Formula (4.1) thus follows from applying this Poincaré inequality in (4.3). □

To illustrate the long-time decay of solutions in the periodic case, let $u^0(x)$ be the Gaussian profile given by (3.4) and let $\delta = 10^{-3}$, $\varepsilon = 2 \times 10^{-4}$, and $p = 5$. This is the same initial condition used to generate the data in Table 4, except the dissipation has been increased by

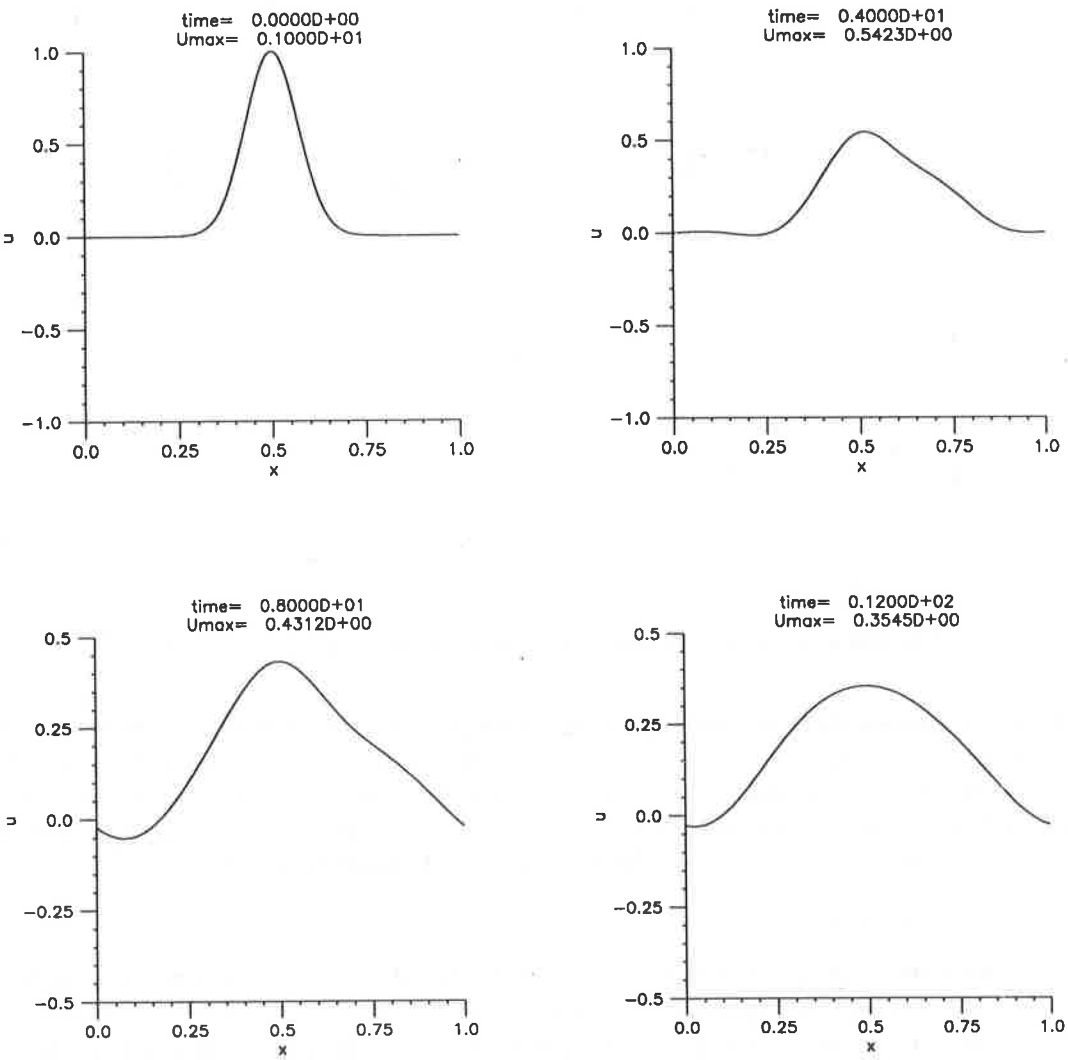

Fig. 3(a). Decay of Gaussian profile with $p = 5$, $\varepsilon = 2 \times 20^{-4}$, $\delta = 10^{-3}$.

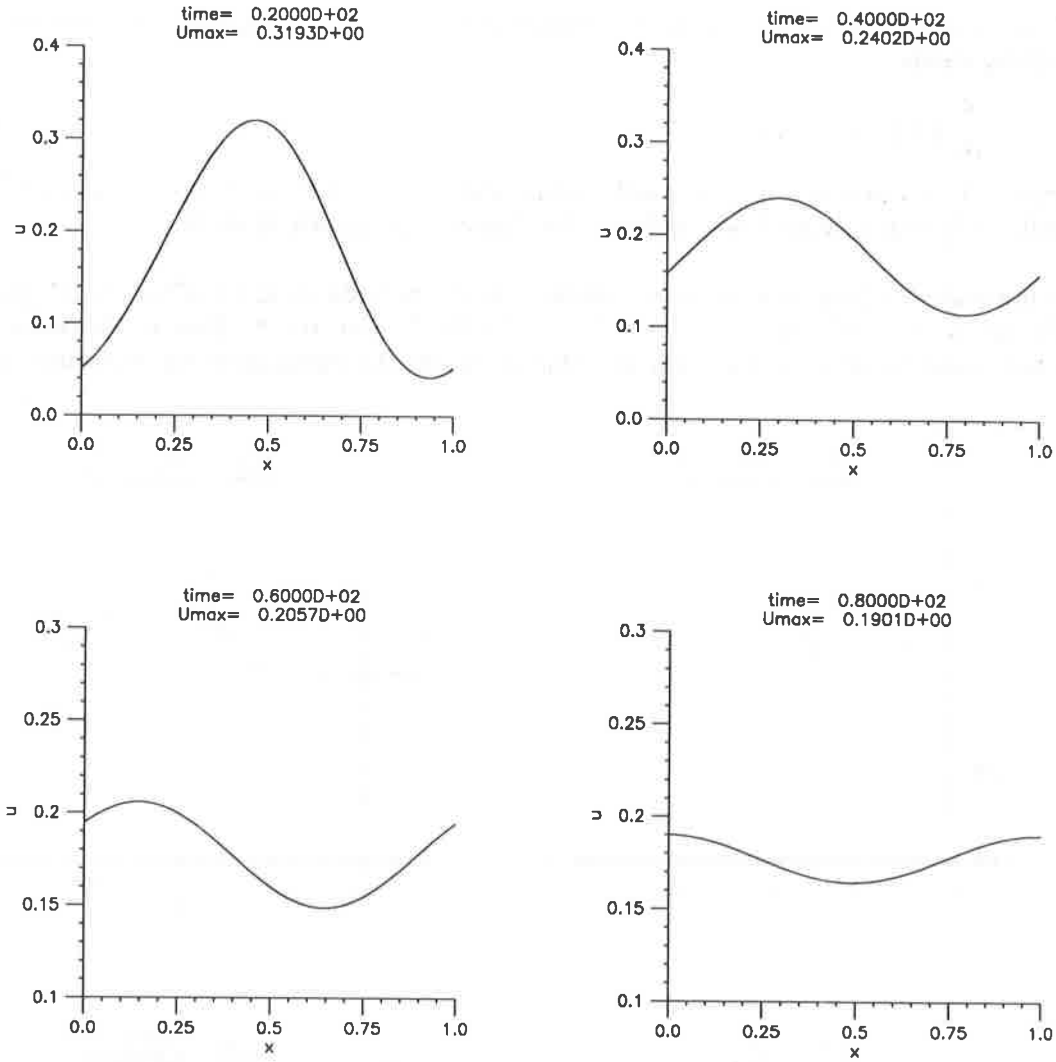

Fig. 3(b). Continued decay of Gaussian profile with $p = 5$, $\varepsilon = 2\times10^{-4}$, $\delta = 10^{-3}$.

one order of magnitude. The corresponding solution is pictured in Fig. 3. Note that for this initial condition, we have $u^* = 0.1772$ and that the solution does indeed decay toward this value. Furthermore, computing various norms of the function $v(x, t) = u(x, t) - u^*$ for several values of t allows us to ascertain approximately the rates at which the norms decay. Letting $M(t)$ stand for any norm of $v(x, t)$, the rate of decay is given by μ where

$$M(t) \sim C\,\mathrm{e}^{-\mu t} \quad \text{as } t \to \infty.$$

The numerical determination of these rates are reported in Table 8 at time increments of 10. They are all observed to approach the value $4\pi^2\delta = 0.3947842 \times 10^{-1}$. This is the value predicted in Proposition 4.1 for the convergence in the L_2-norm. It is interesting that *all* the rates approach the same value as t becomes large. This is a numerical indication that the

Table 8
Decay rates, Gaussian profile, $p=5$, $\varepsilon=2\times10^{-4}$, $\delta=10^{-3}$

t	L_2	L_4	L_5	L_6	L_7	L_∞	$L_{2,D}$	$L_{\infty,D}$
10	0.4197(−1)	0.5131(−1)	0.5357(−1)	0.5508(−1)	0.5614(−1)	0.5708(−1)	0.5407(−1)	0.5719(−1)
20	0.3979(−1)	0.4020(−1)	0.4027(−1)	0.4028(−1)	0.4027(−1)	0.3192(−1)	0.4018(−1)	0.4510(−1)
30	0.3951(−1)	0.3961(−1)	0.3966(−1)	0.3971(−1)	0.3976(−1)	0.4457(−1)	0.3969(−1)	0.4098(−1)
40	0.3948(−1)	0.3949(−1)	0.3949(−1)	0.3949(−1)	0.3949(−1)	0.3826(−1)	0.3947(−1)	0.3935(−1)
50	0.3948(−1)	0.3949(−1)	0.3949(−1)	0.3949(−1)	0.3949(−1)	0.4002(−1)	0.3948(−1)	0.3924(−1)
60	0.3948(−1)	0.3948(−1)	0.3948(−1)	0.3948(−1)	0.3948(−1)	0.3942(−1)	0.3948(−1)	0.3939(−1)
70	0.3948(−1)	0.3948(−1)	0.3948(−1)	0.3948(−1)	0.3948(−1)	0.3956(−1)	0.3948(−1)	0.3954(−1)
80	0.3948(−1)	0.3948(−1)	0.3948(−1)	0.3948(−1)	0.3948(−1)	0.3950(−1)	0.3948(−1)	0.3947(−1)

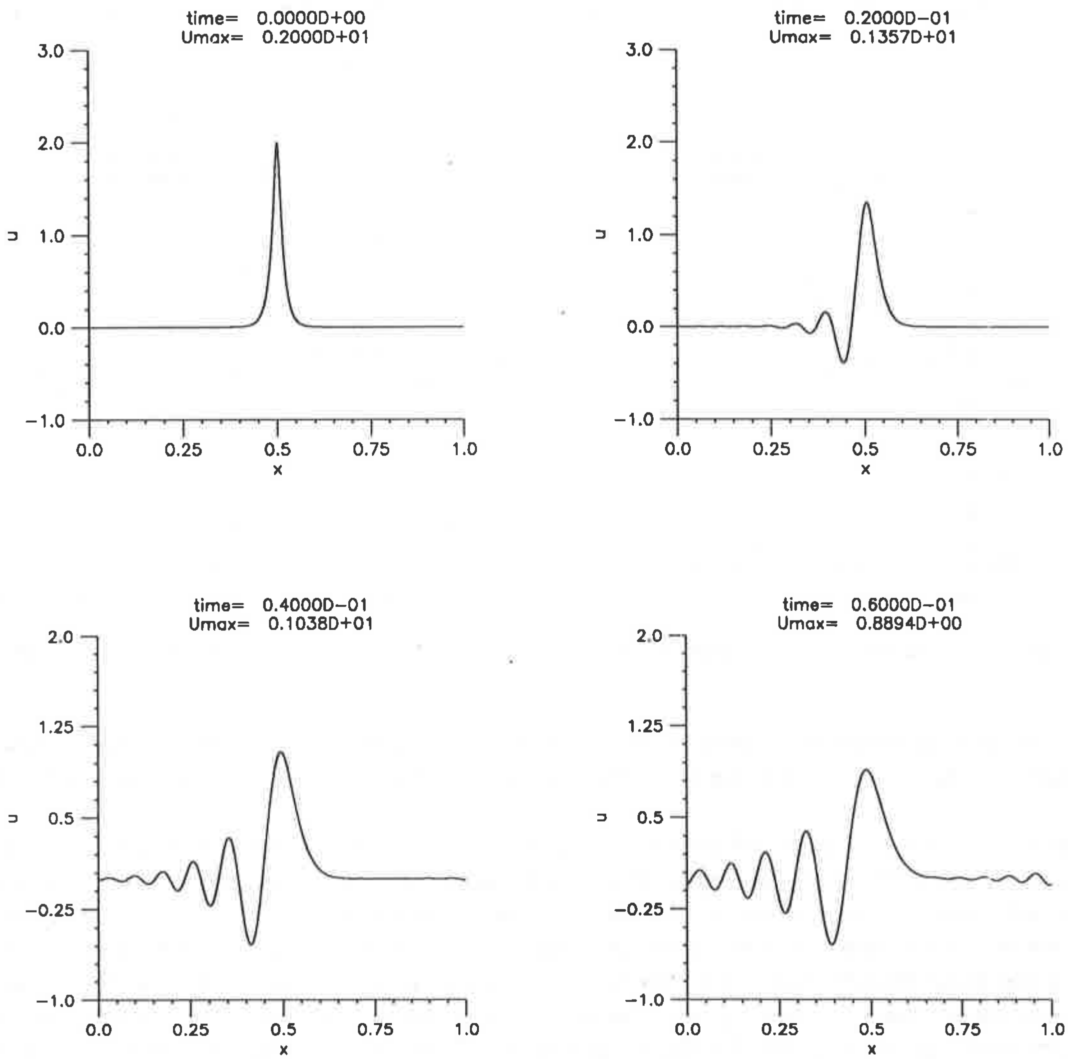

Fig. 4(a). Breakup of solitary-wave solution with $p=6$, $A=2$, $\varepsilon=5\times10^{-4}$, $\delta=5\times10^{-4}$.

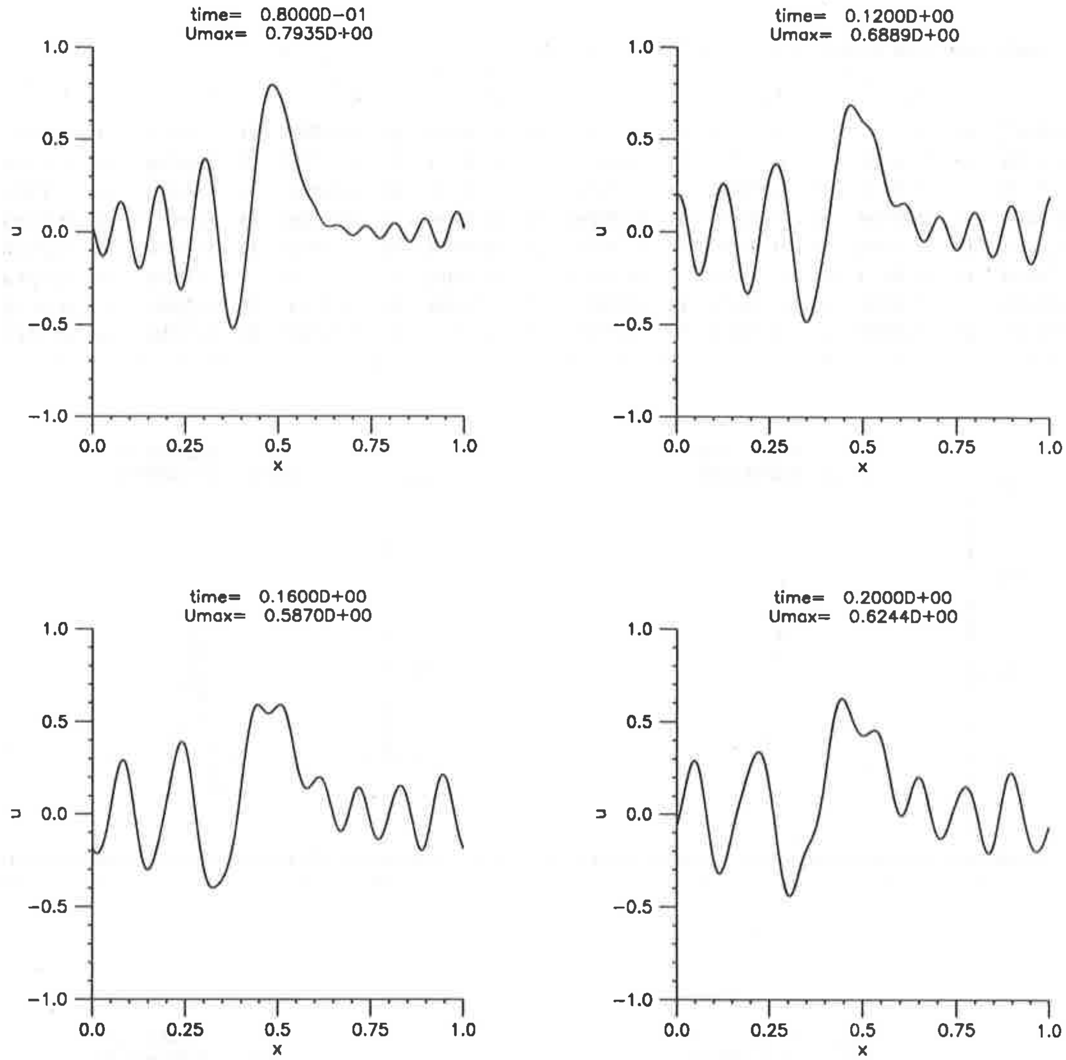

Fig. 4(b). Continuation of breakup of solitary-wave solution with $p = 6$, $A = 2$, $\epsilon = 5\times10^{-4}$, $\delta = 5\times10^{-4}$.

solutions are approaching eigenfunctions of the operator $-\delta D_{xx}$ with periodic boundary conditions, a fact proved by Biler [7] in the case $p < 2$. This issue will receive more attention in [11].

Our last example is pictured in Fig. 4. These graphs show the numerical approximation of the solution of (1.2) corresponding to $p = 6$ with initial data an exact solitary wave of amplitude 2, but with substantial dissipation. In this case the dissipation is more than ample to prevent instabilities of the solitary wave from growing. The immediate effect of the dissipation is to form a highly oscillatory tail which, due to the periodicity, quickly interacts with the remnant of the main pulse which has not appreciably moved. Continuing this run over a much longer time horizon shows the various modes decaying with the high modes dying out first. Eventually the solution becomes very similar to that in Fig. 3 and approaches a constant which, for this initial condition is $u^* = 0.7184 \times 10^{-1}$. More details on the rates of decay and the shape and speed of the travelling-wave solutions will be presented in [11].

References

[1] L. Abdelouhab, J.L. Bona, M. Felland and J.-C. Saut, Nonlocal models for nonlinear dispersive waves, *Phys. D* 40 (1989) 360–392.

[2] J.P. Albert, J.L. Bona and M. Felland, A criterion for the formation of singularities for the generalized Korteweg–de Vries equation, *Mat. Apl. Comput.* 7 (1988) 3–11.

[3] C.J. Amick, J.L. Bona and M.E. Schonbek, Decay of solutions of some nonlinear wave equations, *J. Differential Equations* 81 (1989) 1–49.

[4] G.A. Baker, V.A. Dougalis and O.A. Karakashian, Convergence of Galerkin approximations for the Korteweg–de Vries equation, *Math. Comp.* 40 (1983) 419–433.

[5] T.B. Benjamin, Lectures on nonlinear wave motion, in: A. Newell, ed., Lectures in Applied Mathematics 15 (American Mathematical Society, Providence, RI, 1974) 3-47.

[6] T.B. Benjamin, J.L. Bona and J.J. Mahony, Model equations for long waves in nonlinear, dispersive media, *Philos. Trans. Roy. Soc. London Ser. A* 272 (1972) 47–78.

[7] P. Biler, Large-time behaviour of periodic solutions of two dispersive equations of Korteweg–de Vries–Burgers type, *Bull. Polish Acad. Sci.* 32 (1984) 401–405.

[8] J.L. Bona, Convergence of periodic wavetrains in the limit of large wavelength, *Appl. Sci. Res.* 37 (1981) 21–30.

[9] J.L. Bona, V.A. Dougalis and O.A. Karakashian, Fully-discrete Galerkin methods for the Korteweg–de Vries equation, *Comput. Math. Appl.* 12A (7) (1986) 859–884.

[10] J.L. Bona, V.A. Dougalis, O.A. Karakashian and W.R. McKinney, Conservative, high-order schemes for the generalized Korteweg–de Vries equation (to appear).

[11] J.L. Bona, V.A. Dougalis, O.A. Karakashian and W.R. McKinney, The effect of dissipation on the evolution of solutions of the generalized Korteweg–de Vries equation (in preparation).

[12] J.L. Bona, W.G. Pritchard and L.R. Scott, An evaluation of a model equation for water waves, *Philos. Trans. Roy. Soc. London Ser. A* 302 (1981) 457–510.

[13] J.L. Bona, P.E. Souganidis and W.A. Strauss, Stability and instability of solitary waves of KdV type, *Proc. Roy. Soc. London Ser. A* 411 (1987) 395–412.

[14] K. Dekker and J.G. Verwer, eds., *Stability of Runge–Kutta Methods for Stiff Nonlinear Differential Equations,* CWI Monographs 2 (North-Holland, Amsterdam, 1984).

[15] D. Dix, Decay of solutions to the Benjamin–Ono–Burgers equation, Ph.D. Thesis, University of Chicago, Chicago, IL (1988).

[16] H. Grad and P.N. Hu, Unified shock profile in a plasma, *Phys. Fluids* 10 (1967) 2596–2602.

[17] A. Jeffrey and T. Kakutani, Weak nonlinear dispersive waves: a discussion centered around the Korteweg–de Vries equations, *SIAM Rev.* 14 (1972) 582–643.

[18] R.S. Johnson, A nonlinear equation incorporating damping and dispersion, *J. Fluid Mech.* 42 (1970) 49–60.

[19] R.S. Johnson, Shallow water waves on a viscous fluid—the undular bore, *Phys. Fluids* 15 (1972) 1693–1699.

[20] O.A. Karakashian and W.R. McKinney, On optimal high order in time approximations for the Korteweg–de Vries equation, *Math. Comp.* 55 (1990) 473–496.

[21] T. Kato, On the Korteweg–de Vries equation, *Manuscripta Math.* 28 (1979) 89–99.

[22] T. Kato, On the Cauchy problem for the (generalized) Korteweg–de Vries equation, in: *Studies in Applied Mathematics.* Advances in Mathematics, Supplementary Studies 8 (Academic Press, New York, 1983) 93–130.

[23] E. Schechter, Well-behaved evolutions and the Trotter product formulas, Ph.D. Thesis, University of Chicago, Chicago, IL (1978).

[24] A.C. Scott, F.Y.F. Chu and D.W. McLaughlin, The soliton: a new concept in applied science, *Proc. IEEE* 61 (1973) 1443–1483.

[25] W.A. Strauss, Dispersion of low-energy waves for two conservative equations, *Arch. Rational Mech. Anal.* 55 (1974) 86–92.